Magnetic domains in epitaxial ordered FePd(001) thin films with perpendicular magnetic anisotropy

V. Gehanno and A. Marty
Service de Physique des Matériaux et Microstructures/Département de Recherche Fondamentale sur la Matière Condensée/CEA, 38 054 Grenoble, France

B. Gilles
Laboratoire de Thermodynamique et Physico-Chimie Métallurgiques/CNRS, Boîte Postale 75, 38 042 St Martin d'Hères, France

Y. Samson
Service de Physique des Matériaux et Microstructures/Département de Recherche Fondamentale sur la Matière Condensée/CEA, 38 054 Grenoble, France

(Received 25 November 1996)

Small magnetic domains (70 nm) have been observed by magnetic force microscopy in ordered FePd thin films grown by molecular-beam epitaxy. The layers exhibit a perpendicular magnetic anisotropy induced by uniaxial $L1_0$ [CuAu(I)-type] chemical ordering. The magnetization curves show that the easy magnetization axis is perpendicular to the film plane and their interpretation with a micromagnetic model leads to the correct size of the domains. [S0163-1829(97)00318-4]

Magnetic layers with a high perpendicular anisotropy appear as an attractive solution to increase the information density in magneto-optic recording media. Currently, longitudinal magnetic recording systems reach densities of 10 Gbits/in^2, while computer simulations based on the perpendicular magnetic recording (PMR) mode anticipate densities of 300 Gbits/in^2 for the 21st century.[1] To achieve the PMR configuration, many efforts are devoted to the materials exhibiting a uniaxial magnetic anisotropy. To take advantage of the magnetocrystalline anisotropy, it is critical to control the elaboration conditions so that the direction of the easy axis of magnetization is perpendicular to the film plane. Recently, research focused on binary metallic alloys developing a uniaxial magnetic anisotropy associated with a chemical ordering phase transition. In this way, magnetic layers of ordered PtCo and PtFe with perpendicular magnetic anisotropy have been elaborated.[2,3] The magnetocrystalline anisotropy was strong enough to exceed the demagnetizing field which tends to confine the magnetization in the plane of the layers. Since the chemical ordering was shown to be accompanied by a large enhancement of the Kerr rotation in these layers, this type of material is very promising for magneto-optic applications.

The FePd system exhibits a phase transition at the equiatomic composition around 920 K between a disordered face-centered-cubic phase and an $L1_0$ [CuAu(I)-type] ordered tetragonal structure.[4] This ordered structure consists of alternating planes of Fe and Pd atoms so that it has only one fourfold symmetry axis which is expected to be an easy magnetization axis.[5,6] In this letter, we report on the observation of nanometric magnetic domains in ordered FePd thin films having the easy axis normal to the surface. The crystallographic structure of the metallic layer was investigated in detail with x-ray-diffraction (XRD) experiments as well as transmission electron microscopy (TEM) observations. The magnetic properties were studied by standard vibrating sample magnetometry (VSM) and magnetic force microscopy (MFM). We show that the models developed in the 1960's for garnet materials[7] may be applied to ordered metallic alloys with nanometric magnetic domains.

The FePd thin film was deposited onto a Pd(001)-oriented surface held at a temperature of 600 K during the deposition of the alloy. We found that this temperature, being considerably lower than the bulk order-disorder transition temperature, is high enough to induce ordering at the surface during deposition. Pd was chosen as the buffer layer since its lattice parameter has a misfit of 1% with the in-plane lattice parameter of the ordered FePd phase.[8] Indeed the minimization of the epitaxial strains in the growing layer should favor the formation of the ordered phase with the fourfold-symmetry axis parallel to the growth axis.

The samples were prepared by molecular-beam epitaxy (MBE) under ultrahigh vacuum (10^{-7} Pa). A 2-nm seed layer of Cr was deposited onto a MgO (001)-oriented surface in order to induce the epitaxial growth of the 60-nm single-crystal Pd buffer layer. During a 10 min annealing at 700 K the reflection high-energy electron-diffraction (RHEED) pattern transformed from spots to rods indicating the smoothing of the Pd(001)-oriented surface.[9] Then the buffer layer was cooled down to 600 K and a 50-nm equiatomic FePd layer was codeposited at the rate of 0.2 atomic monolayer per second. This was performed by simultaneous evaporation of pure Fe and pure Pd from two independently controlled electron-beam sources. The incident fluxes of Fe and Pd were each set to 0.1 atomic monolayer per second. Each electron-beam source was controlled by a quartz crystal sensor calibrated using the RHEED oscillations induced by the pseudomorphic growth of pure Fe and pure Pd on a Pd(001) surface. The layer was covered by a 2-nm Pd capping to prevent from oxidation. The RHEED diagram revealed the cube-on-cube epitaxial relationship (001)[001]Pd/(001)[001]FePd with no visible relaxation of the in-plane

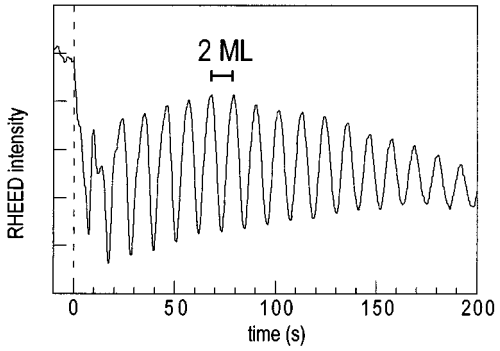

FIG. 1. RHEED intensity oscillations during the codeposition of FePd at 600 K on the Pd(001) surface. The period of the oscillations corresponds to the time required to form two atomic layers of alloy.

FePd lattice parameter occurring during deposition. The intensity of the specular reflection of the electron beam on the surface of the growing layer is presented in Fig. 1. We observe oscillations with a period corresponding to the time required for the deposition of 2 atomic layers, indicating that the growth proceeds bilayer by bilayer. Since the $L1_0$ ordered structure has a spatial period of 2 monolayers, this suggests that chemical ordering is occurring at the surface during the growth. One may note that the double layer period is commonly observed during the epitaxial growth of GaAs by MBE.[10] The explanation is quite similar: one oscillation corresponds to the growth of one complete layer of Ga, plus one complete layer of As.

The evidence for the $L1_0$ ordering is given by a transmission electron microscopy diffraction pattern of a plan view sample [Fig. 2(a)]. In addition to the {200} and {220} fundamental reflections of the face-centered-cubic lattice, strong and sharp {110} superlattice spots are present, indicating $L1_0$ ordering along the growth direction. Moreover, from the absence of the {100} reflections, we deduce that the ordering is uniaxial with only one of the three possible variants of the $L1_0$ ordered structure.

For comparison, we present the diffraction pattern of a sample codeposited at 300 K [Fig. 2(b)]. It differs from the precedent pattern by the absence of the {110} superlattice reflections. This reveals that the disordered face-centered-cubic phase has been obtained during the deposition at 300 K. We conclude that the temperature of the substrate during the deposition is a critical parameter that controls the long-range order in the growing layer.

A quantitative measurement of the degree of order has been obtained from XRD experiments. The symmetric XRD scans (Fig. 3) exhibit the (002) fundamental peak for the MgO substrate, the Pd buffer layer and the FePd layer. The presence of an intense (001) superlattice reflection for the alloy layer confirms the $L1_0$ ordering. The long-range order parameter defined as $S=|n_{\mathrm{Fe}}-n_{\mathrm{Pd}}|$, where $n_{\mathrm{Fe(Pd)}}$ stands for the site occupancy on the Fe(Pd) sublattice, is estimated from the ratio of the integrated intensities of any fundamental and superlattice reflection.[11] For the calculation we took into account the Lorentz-polarization correction factor and the thin layer effect. We used tabulated values for the atomic scattering factors.[12] The integration of the two superlattice diffraction peaks (001) and (003) and the two fundamental

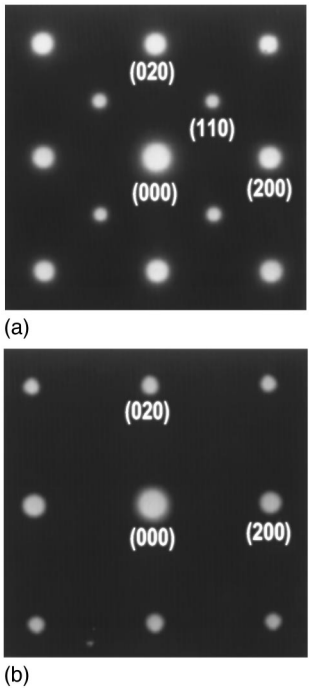

FIG. 2. TEM diffraction pattern taken with the electron beam parallel to the (001) growth axis: (a) codeposition at 600 K, (b) codeposition at 300 K. The two diagrams exhibit the cubic symmetry with the {200} and {020} spots corresponding to the fundamental reflections of the face-centered-cubic lattice. The pattern corresponding to the sample codeposited at 600 K exhibits {110} spots: they result from the $L1_0$ ordering with the direction of the fourfold-symmetry axis along the growth direction. Note the absence of the (100) and (010) spots corresponding to the two other possible orientations of the ordered phase, i.e., with the fourfold symmetry axis in the plane of the thin film parallel to the (100) or (010) axis.

reflections (002) and (004) allowed us to extract values for both the Debye-Waller factors and the long-range order parameter estimated at $S=0.8\pm0.1$. Since S ranges from 0 for a completely disordered film to 1 for a perfectly ordered film, this experiment demonstrates the high degree of chemical order in the layer.

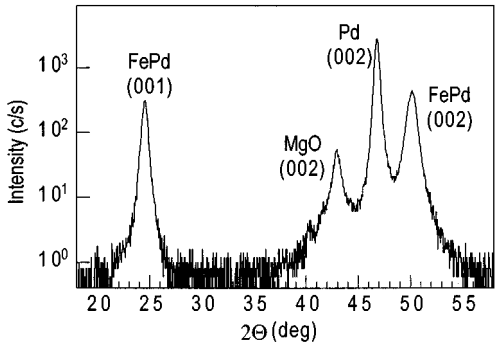

FIG. 3. Θ–2Θ x-ray-diffraction scan along the (001) direction, i.e., the growth direction, taken with the CuAu ($K\alpha$) radiation. The (002) peaks for the MgO substrate, the Pd buffer layer and the FePd layer correspond to the fundamental reflection of the face-centered-cubic lattice. The (001) peak for FePd results from the CuAu(I) ordering with the fourfold-symmetry axis of the structure normal to the film.

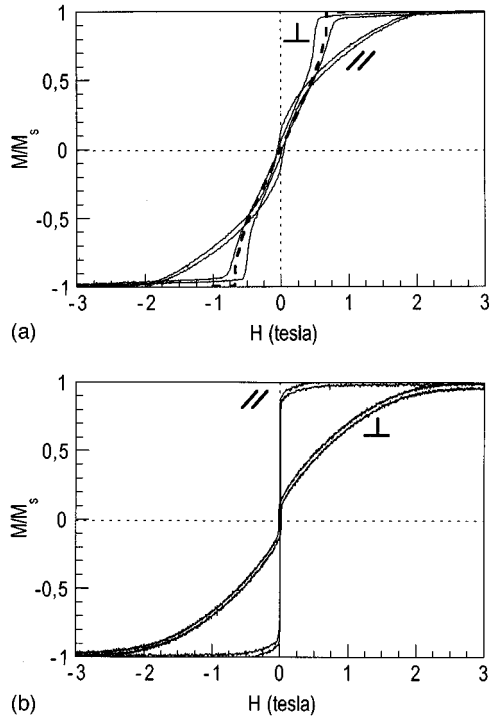

FIG. 4. The unbroken lines represent the experimental hysteresis loops measured on a VSM with the external field parallel (∥) or perpendicular (⊥) to the film plane. (a) The sample was codeposited at 600 K: it is more easily magnetized when the field is applied out of the plane of the layer. The shape of the curve with the out-of-plane external field is characteristic of the presence of magnetic domains. The broken line corresponds to the curve calculated according to the model of Kooy and Enz (Ref. 7) to fit the experiment. (b) The sample was codeposited at 300 K: it is more easily magnetized when the field is applied in the plane of the layer.

The magnetization curves [Fig. 4(a)] were measured using a VSM with the external field either parallel or perpendicular to the layer plane. We deduce from the measurements that the saturation magnetization M_s is 1200 ± 100 emu/cm^3 which is in agreement with the values given in the literature for bulk FePd ordered alloys.[5,6] The magnetization curves clearly show that the sample is more easily magnetized when the field is applied perpendicularly to the layer, indicating a preferred orientation of the magnetization out-of-the plane. For comparison, we present the magnetization curves of the sample codeposited at 300 K [Fig. 4(b)]. This thin layer of the disordered phase is more easily magnetized when the field is applied in the plane of the layer: this demonstrates that, due to the absence of uniaxial magnetocrystalline anisotropy, the minimization of the demagnetizing energy keeps the magnetization in the plane of the layer under zero field. For the sample codeposited at 600 K, the uniaxial magnetocrystalline anisotropy resulting from the $L1_0$ ordering exceeds the demagnetizing factor: this results in a perpendicularly magnetized thin film. The comparison between the two samples clearly reveals the importance of the chemical degree of order to obtain perpendicular anisotropy. A method for measuring the uniaxial anisotropy constant K_u has been developed by Druyvesteyn, Dorleijn, and Rijnierse.[13] They obtained a relation between the in-plane saturation field H_s^{para} and the uniaxial anisotropy field $H_k = 2K_u/M_s$ depending on the value of a characteristic magnetic length l of the material. They showed that, whatever the value of l, H_k is always larger than H_s^{para} leading in our case to 1.2×10^7 erg/cm^3 as a lower limit for the uniaxial anisotropy constant K_u whose value will be estimated below. The contribution of the magnetoelastic effects was estimated to be less than 10^6 erg/cm^3 according to the deformation induced by the epitaxial strains and the magnetoelastic constants.[14] Therefore we can consider that the measured value of the anisotropy results only from the magnetocrystalline anisotropy. Finally the present experiment shows that it is sufficient to exceed the demagnetizing factor. Moreover the shape of the magnetization curve with the perpendicular field reveals that the sample is not homogeneously magnetized, since this would give a square-shaped hysteresis loop, but it is divided into magnetic domains, the direction of the magnetization being alternatively up and down in the layer.

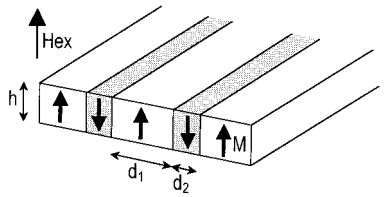

FIG. 5. Schematic representation of the domain structure postulated for the modeling.

This kind of shape and the one already observed in thin layers of garnet materials which also exhibit perpendicular anisotropy are very alike. Kooy and Enz proposed a model in the 1960's to explain the observed domain size in these materials.[7] We can use the same expression for the total energy of the layer as composed of the wall energy E_w, the demagnetizing energy E_D, and the energy E_H of the sample in the external field H applied perpendicularly to the layer. The model assumes that the domain structure consists of straight domains with the demagnetization field as well as the 180° Bloch walls perpendicular to the surface (Fig. 5). The parameters d_1 and d_2 stand for the widths of the domains where the magnetization is parallel or antiparallel to the direction of the applied field and h is the thickness of the layer. Under these assumptions the wall energy density E_w in the layer is $E_w = \sigma_w 2h/(d_1+d_2)$ where $\sigma_w = 4\sqrt{AK_u}$ is the wall-surface energy density and A is the exchange constant of the material. The energy density E_H of the sample in the applied field H is given by $E_H = -hHM$ where $M = M_s(d_1 - d_2)/(d_1+d_2)$ is the resultant magnetization of the sample and M_s is the saturation magnetization of the material. The demagnetizing energy density E_D of the domain configuration is given by

$$E_D = 2\pi h M^2 = \frac{2\sqrt{\mu}}{1+\sqrt{\mu}} \frac{8}{\pi^2} M_s^2 \frac{h}{\alpha} \sum_{n=1}^{\infty} \frac{1}{n^3} \sin^2\left[\frac{n\pi}{2}\left(1+\frac{M}{M_s}\right)\right] \times [1-\exp(-2n\pi\alpha)],$$

where $\alpha = h\sqrt{\mu}/(d_1+d_2)$. It includes the μ effect ($\mu = 1 + 2\pi M_s^2/K_u$) due to the fact that the uniaxial anisotropy energy K_u is only slightly higher than the demagnetizing energy $2\pi M_s^2$.[15]

This model based on a postulated domain structure allows us to evaluate the contribution of the different energy terms. It shows how the formation of magnetic domains is induced by the diminution of the magnetostatic energy. The width of the stripes when no external field is applied follows from the equilibrium between the wall energy E_w and the magnetostatic energy E_D. Furthermore hysteresis loops with normal external fields can be calculated by minimizing the total energy of the system $E_{\text{tot}}=E_w+E_D+E_H$ with respect to the domain size. Both the stripe width under zero field and the calculated hysteresis curve depend on the parameter h/l where $l=\sigma_w/(4\pi M_s^2)$ is the characteristic material length. We have fitted the experimental magnetization curve by varying the parameter h/l and we found $h/l=10$ for the calculated curve reproduced in Fig. 4. This value is used to estimate the uniaxial magnetic constant according to the model of Druyvesteyn, Dorleijn, and Rijnierse.[13] This yields $K_u=(1.5\pm0.2)10^{7}$ erg/cm^3. As expected according to the high value of the long-range order parameter, K_u is only slightly lower than the magnetic anisotropy constant of $(2-3)\ 10^7$ erg/cm^3 given in the literature for the bulk ordered structure.[5,6] The value of the characteristic length gives also the theoretical width of the stripes at equilibrium with no external field: 50 nm.

Such small domains were indeed directly visible by MFM. Measurements were performed using a nanoscope IIIa from Digital Instruments, in the ac mode where the force gradient (second derivative of the magnetic field) between a magnetic tip and the sample is detected.[16] The as-grown sample exhibits highly interconnected stripes corresponding to the alternate up and down orientations of the magnetization (Fig. 6). Despite their small size, the domains are imaged with a high contrast which allows a precise determination of their well-defined characteristic width: 70 ± 5 nm. This size is of the same order of magnitude than the one predicted by the model.

Magnetic domains so small have been recently observed by Hehn *et al.* in perpendicularly magnetized cobalt thin films.[17] In this system, the uniaxial magnetic anisotropy resulting from the magnetocrystalline anisotropy of the Co phase is lower than the demagnetizing energy: $\hat{K}=K_u/2\pi M_s^2=0{,}35$. Consequently, the magnetization lies in the plane of the layer when the thickness falls below about 30 nm. This is not expected in the FePd system where the magnetic anisotropy induced by the chemical ordering is significantly larger than the demagnetizing energy: $\hat{K}=1.66$. As a result, perpendicularly magnetized FePd thin films can be obtained in a wide thickness range. This should allow an extensive study of the domain configuration with respect to the layer thickness. Current research efforts are devoted to this task.

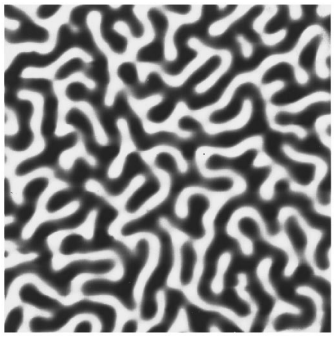

FIG. 6. Magnetic domain structure of the ordered FePd thin film observed with a MFM. Taken in the ac mode this image maps the phase shifts in the cantilever oscillations. Dark and bright areas correspond to up and down perpendicularly magnetized domains. The image size is 2 μm$\times$2 μm.

The MFM image demonstrates that nanometric magnetic domains are the lowest energy configuration in thin FePd layers having the magnetization perpendicular to the film plane. The required magnetic anisotropy is induced by the high uniaxial $L1_0$ chemical order obtained during the MBE growth. Since the growth process leads to only one variant and thus to a purely perpendicular anisotropy axis, the quantitative analysis of the structural state of order and magnetic configuration is greatly simplified. Therefore this epitaxial system opens opportunities to investigate the relationship between the magnetic anisotropy, the magnetic configuration, and structural parameters such as the chemical order.

The authors would like to thank P. Auric, A. Chamberod, B. Pras, G. Patrat, J. Eymery, and M. Dynna for stimulating discussions and helpful assistance.

[1] J. C. Lodder, MRS Bull. **20**, 59 (1995).
[2] B. M. Lairson and B. M. Clemens, Appl. Phys. Lett. **63**, 1438 (1993).
[3] A. Cebollada *et al.*, Phys. Rev. B **50**, 3419 (1994).
[4] For more information on the CuAu(I)-type structure, see for example, F. C. Nix and W. Shockley, Rev. Mod. Phys. **10**, 1 (1938).
[5] N. Miyata, H. Asami, T. Misushima, and K. Sato, J. Phys. Soc. Jpn. **59**, 1817 (1990).
[6] B. Zhang and W. A. Soffa, Scr. Metall. Mater. **30**, 683 (1994).
[7] C. Kooy and U. Enz, Philips Res. Rep. **15**, 7 (1960).
[8] E. Raub, H. Beeskow, and O. Loebich, Z. Metallkd. **54**, 549 (1963).
[9] J. E. Maham, K. M. Geib, G. Y. Robinson, and R. G. Long, J. Vac. Sci. Technol. A **8**, 3692 (1990).
[10] For instance, J. J. Harris, B. A. Joyce, and P. J. Dobson, Surf. Sci. **108**, L444 (1981).
[11] B. E. Warren, *X-ray Diffraction* (Dover, New York, 1990), pp. 206–250.
[12] For tabulated values of the atomic scattering factors, see the *International Tables for X-Ray Crystallography*, 2nd ed. (Lonsdale, Birmingham, England, 1968), Vol. 3, pp. 201–216.
[13] W. F. Druyvesteyn, J. W. F. Dorleijn, and P. J. Rijnierse, J. Appl. Phys. **44**, 2397 (1973).
[14] N. Miyata, T. Kamimori, and M. Goto, J. Phys. Soc. Jpn. **55**, 2037 (1986).
[15] H. J. Williams, R. M. Bozorth, and W. Shockley, Phys. Rev. **75**, 155 (1949).
[16] E. D. Dahlberg and J. G. Zhu, Phys. Today **48** (4), 34 (1995).
[17] M. Hehn, S. Padovani, K. Ounadjela, and J. P. Bucher, Phys. Rev. B **54**, 3428 (1996).